



This is a repository copy of *Maximizing the translational potential of neurophysiology in amyotrophic lateral sclerosis: a study on compound muscle action potentials*.

White Rose Research Online URL for this paper:

<https://eprints.whiterose.ac.uk/222311/>

Version: Published Version

Article:

McKinnon, S., Qiang, Z., Keerie, A. et al. (4 more authors) (2025) Maximizing the translational potential of neurophysiology in amyotrophic lateral sclerosis: a study on compound muscle action potentials. *Amyotrophic Lateral Sclerosis and Frontotemporal Degeneration*. ISSN 2167-8421

<https://doi.org/10.1080/21678421.2024.2448540>

Reuse

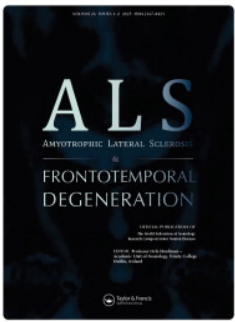
This article is distributed under the terms of the Creative Commons Attribution-NonCommercial-NoDerivs (CC BY-NC-ND) licence. This licence only allows you to download this work and share it with others as long as you credit the authors, but you can't change the article in any way or use it commercially. More information and the full terms of the licence here: <https://creativecommons.org/licenses/>

Takedown

If you consider content in White Rose Research Online to be in breach of UK law, please notify us by emailing eprints@whiterose.ac.uk including the URL of the record and the reason for the withdrawal request.



eprints@whiterose.ac.uk
<https://eprints.whiterose.ac.uk/>



Amyotrophic Lateral Sclerosis and Frontotemporal Degeneration

ISSN: (Print) (Online) Journal homepage: www.tandfonline.com/journals/iafd20

Maximizing the translational potential of neurophysiology in amyotrophic lateral sclerosis: a study on compound muscle action potentials

Scott McKinnon, Zekai Qiang, Amy Keerie, Tyler Wells, Pamela J. Shaw, James J. P. Alix & Richard J. Mead

To cite this article: Scott McKinnon, Zekai Qiang, Amy Keerie, Tyler Wells, Pamela J. Shaw, James J. P. Alix & Richard J. Mead (22 Jan 2025): Maximizing the translational potential of neurophysiology in amyotrophic lateral sclerosis: a study on compound muscle action potentials, Amyotrophic Lateral Sclerosis and Frontotemporal Degeneration, DOI: [10.1080/21678421.2024.2448540](https://doi.org/10.1080/21678421.2024.2448540)

To link to this article: <https://doi.org/10.1080/21678421.2024.2448540>



© 2025 The Author(s). Published by Informa UK Limited, trading as Taylor & Francis Group.



[View supplementary material](#)



Published online: 22 Jan 2025.



[Submit your article to this journal](#)



Article views: 35



[View related articles](#)



[View Crossmark data](#)

RESEARCH ARTICLE

Maximizing the translational potential of neurophysiology in amyotrophic lateral sclerosis: a study on compound muscle action potentials

SCOTT MCKINNON^{1*}, ZEKAI QIANG^{1*}, AMY KEERIE¹, TYLER WELLS¹,
PAMELA J. SHAW^{1,2}, JAMES J. P. ALIX^{1,2¶} & RICHARD J. MEAD^{1,2¶}

¹Department of Neuroscience, Sheffield Institute for Translational Neuroscience (SITraN), The University of Sheffield, Sheffield, UK and ²Neuroscience Institute, The University of Sheffield, Western Bank, Sheffield, UK

Abstract

Mouse models of amyotrophic lateral sclerosis (ALS) enable testing of novel therapeutic interventions. However, treatments that have extended survival in mice have often failed to translate into human benefit in clinical trials. Compound muscle action potentials (CMAPs) are a simple neurophysiological test that measures the summation of muscle fiber depolarization in response to maximal stimulation of the innervating nerve. CMAPs can be measured in both mice and humans and decline with motor axon loss in ALS, making them a potential translational read-out of disease progression. We assessed the translational potential of CMAPs and ascertained time points when human and mouse data aligned most closely. We extracted data from 18 human studies and compared with results generated from SOD1^{G93A} and control mice at different ages across different muscles. The relative CMAP amplitude difference between SOD1^{G93A} and control mice in tibialis anterior (TA) and gastrocnemius muscles at 70 days of age was most similar to the relative difference between baseline ALS patient CMAP measurements and healthy controls in the abductor pollicis brevis (APB) muscle. We also found that the relative decline in SOD1^{G93A} TA CMAP amplitude between 70 and 140 days was similar to that observed in 12 month human longitudinal studies in APB. Our findings suggest CMAP amplitudes can provide a “translational window”, from which to make comparisons between the SOD1^{G93A} model and human ALS patients. CMAPs are easy to perform and can help determine the most clinically relevant starting/end points for preclinical studies and provide a basis for predicting potential clinical effect sizes.

Keywords: Amyotrophic lateral sclerosis, electrophysiology, mouse model, translational biomarker

Introduction

In amyotrophic lateral sclerosis (ALS), an increasing number of molecules are being taken from preclinical studies into clinical trials. While many therapeutic approaches have been successful in mice but unsuccessful in humans (1–6), both edaravone and the antisense oligonucleotide Tofersen have transitioned into positive human trials from successful preclinical studies (7, 8). While modeling the human disease in mice poses many

problems (9), several models are available which provide a testing platform for different pathophysiological aspects of the disease. These include the ALS-FTD TDP-43^{Q331K} knock-in (10) and transgenic models (11), humanized FUS models (12) and the most widely studied model, the SOD1^{G93A} mouse, which provides a robust, predominantly lower motor neuron phenotype (13, 14). Bacterial artificial chromosome (BAC) transgenic models carrying an ALS C9orf72 allele with

Correspondence: Richard Mead, Department of Neuroscience, Sheffield Institute for Translational Neuroscience (SITraN), The University of Sheffield, 385a Glossop Road, Sheffield S10 2HQ, UK. E-mail: r.j.mead@sheffield.ac.uk; James Alix, Department of Neuroscience, Sheffield Institute for Translational Neuroscience (SITraN), The University of Sheffield, 385a Glossop Road, Sheffield S10 2HQ, UK. E-mail: j.alix@sheffield.ac.uk

*Both authors contributed equally to this work.

¶Both authors contributed equally as senior authors.

 Supplemental data for this article can be accessed online at <https://doi.org/10.1080/21678421.2024.2448540>

(Received 15 July 2024; revised 25 November 2024; accepted 1 December 2024)

ISSN 2167-8421 print/ISSN 2167-9223 online © 2025 The Author(s). Published by Informa UK Limited, trading as Taylor & Francis Group.

This is an Open Access article distributed under the terms of the Creative Commons Attribution-NonCommercial-NoDerivatives License (<http://creativecommons.org/licenses/by-nc-nd/4.0/>), which permits non-commercial re-use, distribution, and reproduction in any medium, provided the original work is properly cited, and is not altered, transformed, or built upon in any way. The terms on which this article has been published allow the posting of the Accepted Manuscript in a repository by the author(s) or with their consent.

DOI: 10.1080/21678421.2024.2448540

a hexanucleotide repeat expansion have shown phenotypes in some laboratories (15) but not others (16).

Despite obvious advantages, relatively few therapeutic candidates have been studied with the same read-out of disease in both preclinical and clinical trials. In the SOD1 model, time to reach end-stage disease (“survival time”) is often used (1, 3, 6), partly because this is a common regulatory requirement in phase III clinical trials (17). However, positive effects on survival can be the result of poor experimental design (18). Evaluation of other outcome measures could provide enhanced insight into treatment effects and may provide a better platform for assessing the potential for positive clinical outcomes. For example, in clinical trials, the most common measure of disease state is the amyotrophic lateral sclerosis functional rating scale-revised (ALSFRS-R) (19). However, while there are measures of symptom severity in mice (e.g. neurological score (14)), these are not directly translatable.

Neurophysiological tools are attractive candidates for translational studies, as the same measurements can be made in both mice and humans. Compound muscle action potential (CMAP) amplitude is one example, representing the balance between motor unit loss and compensatory reinnervation. As a result, CMAP amplitude is less sensitive to motor neuron loss compared to motor unit estimation measures (20–24). However, it is arguably the simplest neurophysiological readout to incorporate into complex preclinical studies.

To explore the potential of neurophysiology to provide a translational biomarker of disease, we have compared CMAP amplitude data collected from a systematic search of the available literature to our own CMAP data from multiple muscles in the SOD1^{G93A} mouse. Our first aim was to assess which muscles and timepoints in the mice align best with ALS patient CMAP data at the time of recruitment into clinical studies. Second, we sought to establish which muscles in SOD1^{G93A} mice demonstrate a decline in CMAP over time that is most similar to that observed in ALS patients.

Methods

Ethics

All *in vivo* studies were carried out in compliance with the Animals (Scientific Procedures) Act 1986 and all work was completed by UK Home Office personal license holders under a UK Home Office project license. All mice were housed and cared for according to the Home Office Code of Practice for the Housing and Care of Animals Used in Scientific Procedures.

Mouse model

Transgenic SOD1^{G93A} C57BL/6 mice have been described previously (14). Mice contain ~23 copies of the human transgene containing the glycine to alanine substitution at amino acid 93 as described by Gurney et al. (13).

Mice were housed in groups of 2–5 mice with *ad libitum* access to food (Envigo, Indianapolis, IN) and water. The temperature was maintained at 21 °C with a 12-hour light/dark cycle.

Genotyping

Mice were identified by ear clipping and genomic extraction using QuickExtract (Lucigen, Middleton, WI) and incubated at 65 °C for 15 minutes and 98 °C for two minutes. Genotyping PCR was performed on extracted DNA in 10 μL Master Mix containing: 2 μL FirePol (Solis BioDyne, Tartu, Estonia); 0.25 μL of 10 μM human SOD1 primers (forward 5'-CATCAGCCCTAATCCATCTGA-3', reverse 5'-CGCGACTAACAATCAAAGTGA-3'); 1 μL of 10 μM control IL2 primers (forward 5'-CTAGGCCACAGAATTGAAAGATC-3', reverse 5'-GTAGGTGGAAATTCTAGCATCATCC-3'); 5 μL of nuclease-free water; and 0.5 μL of template DNA. Following PCR, samples were run on a 2% agarose gel. IL2 and human SOD1 PCR products were visualized at ~320 bp and ~250 bp, respectively.

Electrophysiological recording

Electrophysiological testing was carried out at P70, P105, and P140 in 15 transgenic SOD1^{G93A} C57BL/6 (T) and 15 control C57BL/6 female mice (NT). Since we were interested in recording CMAPs from individual muscles, we decided to use needle recording electrodes rather than ring electrodes as they are able to better isolate the specific muscles. This approach has previously been used for electrophysiological recordings in mice (25–29), with prior publications nearly always referring to the potentials obtained as CMAPs (25–28). It is worth noting that these needle based responses will be influenced by the density of myofibers around the needle. Thus, while they still represent a compound potential, they are a far more localized recording. For simplicity, and to maintain the nomenclature of prior papers referring to these as CMAPs, we have retained this label (CMAP).

Mice were anesthetized using gaseous isoflurane (5% isoflurane, flow rate 4L/min oxygen) and then maintained under gaseous anesthesia (1–2% isoflurane, 0.5L/min oxygen continuous inhalation through a nose cone for the duration of the experiment) as is standard for CMAP recordings in mice (25, 29–31). Monopolar needle recording electrodes (Ambu Neuroline) were placed in either the

tibialis anterior (TA), gastrocnemius, intrinsic foot muscle, or the biceps muscles. A reference electrode was placed into the Achilles tendon area for hind limb recordings, and the wrist for forelimb recordings. A ground electrode was placed in the base of the tail. A pair of stimulating electrodes were placed on the skin above the sciatic nerve for hindlimb recordings and above the musculocutaneous nerve for forelimb recordings as done previously (26, 30, 31). Recordings were made using a Dantec Keypoint Focus EMG system. A 0.1 ms square pulse was used and the current gradually increased to obtain supramaximal CMAP responses. The CMAP amplitude was used to measure the output of the targeted muscles. Data were calculated relative to control non-transgenic (NT) mice at each timepoint and as relative decline from 10 weeks of age. GraphPad Prism version 9.3.1 was used for all preclinical statistical analysis (GraphPad Software, San Diego, CA).

Statistical analysis for mouse data was performed using GraphPad Prism version 9.3.1 (GraphPad Software, San Diego, CA). Data are shown as mean \pm SEM, with the inclusion of all data points where applicable to show the spread of the data. The data were analyzed by two-way repeated measures ANOVA followed by a Šidák multiple comparison test to compare with timepoint differences. Coefficient of variation (CV) shown in Supplemental Figures 3 and 4 was calculated from the pooled variance and pooled standard deviation from all of the studies and so captures both within study and between study variation.

Clinical studies: search strategy

Clinical studies were collated through systematic interrogation of the Medline and EMBASE databases for papers up to June 2022. Additional papers were identified through screening the reference list of returned review articles. The studies were restricted to English language only. The search strategy involved a combination of MeSH Terms and keywords: “motor unit number estimate” OR “compound muscle action potential” OR “motor unit number index” AND “motor neuron disease” OR “amyotrophic lateral sclerosis”. We first searched for papers reporting both patient and healthy volunteer values in the same study. Next, we sought papers reporting patient data longitudinally for 12 months.

Study selection

The full texts across both searches were included for data extraction and synthesis if they reported mean and standard deviation of human CMAP data in individual limb muscles. For the comparison of healthy volunteers and ALS patients, the

presence of a healthy control group at a single time point was required. Studies in which ALS patients were not age and gender matched with healthy controls were excluded. For longitudinal data studies, CMAP values were required up to and including 12 months (32–37).

Data extraction

For each included study, data regarding author, publication year, muscles studied, healthy control inclusion criteria, matching status, diagnostic criteria, ALSFRS-R score, and subgroup stratification were extracted. Sample size, mean with standard differences for age, CMAP amplitudes of individual muscles and disease duration were recorded for both healthy and ALS cohorts.

Synthesis

For single studies, extracted raw means and standard deviation data for each muscle were imported. A random-effects model was deployed for quantitative synthesis to take into account the inter-study heterogeneity from varied subject inclusion criteria and demographics. Pooled means were calculated and 95% confidence intervals were determined using Hartung–Knapp adjustment. Heterogeneity between studies was tested by using Higgins and Thompson’s I^2 statistic. For longitudinal studies, percentage changes with respective standard error of the mean (SEM) in CMAP values from baseline were calculated using the extracted data at each timepoint. A linear mixed effects model with a fixed factor “Time (months)”, random factor “Study”, and dependent variable “Percentage change from baseline” was established in order to assess disease progression over the course of 12 months (38, 39). These analyses were performed using the statistical programme RStudio2022.12.0 + 353 (Posit team, Boston, MA).

Results

Human clinical study selection

A total of 54 unique single time point studies were identified, of which 36 were excluded and 18 included. Reasons for exclusion included: no reported relevant CMAP data ($n = 17$); unmatched for age and/or gender ($n = 12$); individual muscle CMAP not reported and/or not specified ($n = 3$); mean CMAP and standard deviation not reported for individual muscles ($n = 3$); bulbar muscle recording ($n = 1$). CMAP measurements were most frequently reported in abductor pollicis brevis (APB; 15 studies). Abductor digiti minimi (ADM) CMAP amplitude was reported in 11 studies, TA in 3, biceps brachii (BB), abductor hallucis (AH), extensor digitorum brevis (EDB), and flexor carpi ulnaris (FCU) in one study. The

Table 1. Heterogeneity across human studies.

Author	Mean age of healthy controls	Diagnostic criteria	Mean age of ALS patients	Mean disease duration (months)	Mean ALSFRS-R score	Reference number
Wang et al. [40] ^a	51.8 ± 9.6	Awaji-Shima	54 ± 13	10 ± 8	43 ± 5	(40)
			57 ± 15	12 ± 12	41 ± 6	
Paparella et al. [41]	64.38 ± 9.66	Revised El Escorial	66.5 ± 8.74	28.57 ± 19.77	39.28 ± 5.22	(41)
Escorcio-Bezerra et al. [42]	62.6 ± 7.4	Revised El Escorial	62.2 ± 8.5	19.28 ± 11.53	NA	(42)
Kim et al. [43] ^a	59.3 ± 8.6	Revised El Escorial	61 ± 11.5	7.8 ± 7.4	38.9 ± 3.9	(43)
			58.9 ± 11.2	10.5 ± 8.3	36.3 ± 3.3	
Zheng et al. [44]	49.3 ± 9.3	Awaji-Shima	59.1 ± 12.8	16 ± 5.8	NA	(44)
Shibuya et al. [45]	59.9 ± 1.3	Revised El Escorial	61.5 ± 0.8	NA	41.06 ± 0.4	(45)
Singh et al. [46]	25.29 ± 2.3	Revised El Escorial	51.86 ± 9.55	11.14 ± 2.85	NA	(46)
Sharma and Miller [47]	48 ± 4	Revised El Escorial	55 ± 4	28 ± 5	NA	(47)
Min et al. [48]	62.98 ± 8.17	Revised El Escorial	61.57 ± 10.74	19.2 ± 19.73	36.47 ± 6.25	(48)
Jenkins et al. [23]	54.2 ± 15.7	Revised El Escorial	57.1 ± 13.5	16.5 (range 6.25–66.25)	40 ± 4.5	(23)
Sun et al. [49] ^b	55 (Range 45–70)	Revised El Escorial	55 (range 41–76)	NA	NA	(49)
			58 (range 50–71)	NA	NA	
Oguz-Akarsu et al. [50]	44.9 ± 13	Awaji-Shima	53 ± 12.1	13.5 ± 13	38.7 ± 7.2	(50)
Iwai et al. [51] ^a	64.2 ± 1.4	Revised El Escorial	64.6 ± 1.2	13.8 ± 1.2	NA	(51)
			67.8 ± 1.1	18.1 ± 1.7	NA	
Fang et al. [52] ^c	50.9 ± 10.86	Revised El Escorial	47.15 ± 9.56	14.3 ± 6.59	38.2 ± 6.65	(52)
			49.6 ± 8.93	15.1 ± 15.77	40.3 ± 3.33	
Fang et al. [53]	50.9 ± 12.8	Revised El Escorial	52.8 ± 11.4	12 ± 9.6	NA	(53)
Deilami et al. [54]	38 ± 11	Revised El Escorial and Awaji-Shima	39.2 ± 14	53.16 ± 13.2	NA	(54)
Gunes et al. [55]	55.8 ± 12.3	Awaji-Shima	56.2 ± 12.1	9.52 ± 7.6	NA	(55)
Shimizu et al. [56]	65.1 ± 12.3	Revised El Escorial and Awaji-Shima	66.5 ± 9.3	19.2 ± 16.8	39.4 ± 7.5	(56)
Boekestein et al. [57]	Median 62 (Range 49–78)	Revised El Escorial	Median 64 (range 21–77)	Median 20.4 (range 9.6–66)	NA	(57)

^aThe study divided ALS patients into two cohorts: one with normal CMAP amplitude, the other with reduced CMAP amplitude.

^bIn this study, ALS patients were divided by upper limb onset ALS and flail arm syndrome.

^cALS patients were divided based on the presence of weakness and wasting of intrinsic hand muscles.

study characteristics are shown in Table 1. There was significant inter-study heterogeneity with $I^2 \geq 75\%$ across all cohorts, an example of this is shown for APB in Supplementary Figure 1. In addition, 22 full texts were reviewed for longitudinal CMAP amplitude data at various monthly intervals. Eight studies were excluded, mostly due to a lack of relevant electrophysiological data ($n = 6$), one did not report CMAP data for individual muscles. APB and ADM were the most frequent muscles to be assessed longitudinally (7 and 10 studies, respectively).

Finding a starting point in mouse to match human baseline data

Using CMAP amplitude data, we first assessed which muscles in the SOD1^{G93A} mouse model, and at which time points, are most representative of the starting point in human clinical trials. We first compared CMAP data from human papers containing both patients with ALS and healthy volunteers (Table 1). While there was significant heterogeneity across studies, CMAP amplitudes in patients were always reduced relative to healthy controls, with APB demonstrating the biggest

relative difference (Supplementary Figure 1: ALS: 5.6 ± 0.62 mV, healthy controls: 10.64 ± 0.74 mV; percentage decline of 47.31%).

We then examined the differences between SOD1^{G93A} and healthy mice across different muscles and at different ages. Significant differences between SOD1^{G93A} and NT mice were evident from 70 days in the TA and gastrocnemius, 105 days in the intrinsic foot muscle, and 140 days in the BB (Supplementary Figure 2). Data were compared across five studies to evaluate the interstudy variation. CMAP data from SOD1^{G93A} mice demonstrate a CV ranging from 19.52 to 48.97% across the observed timepoints and muscles (Supplementary Figure 3). Non-transgenic mice demonstrated a tighter range in CV, 18.20–35.76% (Supplementary Figure 4), comparable to the 35.6% CV between-subject variation of neurofilament light chain in healthy individual serum (58).

We then compared the mouse data to the human data (Figure 1). This showed that TA and gastrocnemius CMAP amplitudes at P70 in the SOD1^{G93A} mice demonstrated a similar relative difference to ALS patients/healthy controls for the APB muscle. The relative reduction in mouse intrinsic foot muscle CMAP amplitude at P105 was similar to APB and FDI CMAPs in humans. In contrast, BB CMAPs in the mouse did not map well to human data at any of the ages studied. We also investigated if there was a split limb index present in the mouse muscles, similar to the split hand/leg indices observed in human patients (59) but did not find any similar phenomena in mice (Supplementary Figure 5).

How do CMAP amplitudes change over time in mice and humans?

As expected, CMAP amplitudes declined over time in both human and SOD1^{G93A} mice (Figure 2 and Supplemental Figures 6–10, Supplemental Tables 2 and 3). As the mouse data for TA and gastrocnemius at P70 appeared to match the human baseline data in APB, we first compared the relative decline in SOD1^{G93A} and human patients for these muscles (Figure 2). From this analysis, it can be seen that the P140 data in mice matches the 12 month time point in human patients and thus the time frame P70–P140 in the mouse would appear to map well to 12 month human studies. Similar plots for the other muscles are given in the supplementary data (Supplementary Figures 7–10). Of these, SOD1^{G93A} TA also aligned well to human TA (Supplemental Figure 10).

Discussion

In this study, we have attempted to align mouse CMAP data with patient data, in order to optimize

the translational potential of preclinical CMAP data. Our results suggest that there are some muscles and time points in the mice that are a better representation of human data than others. While there are limitations to our approach, these observations can stimulate debate on how best to measure ALS disease progression in preclinical studies.

Despite the difficulties in translating successful preclinical studies into successful clinical trials, animal models, and in particular mouse models, remain an important element of ALS research. Between 2019 and 2022, around 400 papers per year were published using mouse models of ALS (PubMed search: ((mouse models) OR (mouse model)) AND ((motor neuron disease) OR (amyotrophic lateral sclerosis))). While there are a number of challenges facing drug development, clinical relevance of the data generated in preclinical models has been identified as being of key importance (60). There has been a rapid increase in the development and validation of biomarkers for ALS in patients (61, 62). However, the development of preclinical biomarkers has lagged behind the human data, although we note that some clinical biomarkers such as neurofilament levels underwent early preclinical evaluation (63, 64). Neurophysiological measures are one of a number of different approaches that can be applied in both mice and patients. The most obvious example is the extension of the CMAP measurement termed motor unit number estimation (MUNE). There are now several MUNE techniques available for patients and, in mice, older methods such as multi-point and incremental MUNE can be applied (65, 66). We acknowledge that MUNE methods could provide a more sensitive readout of disease state than CMAP amplitude in both mouse models and humans and thus may be preferable when possible. However, as a simple starting point, CMAPs are much easier to perform and can be learnt quickly by scientists whose expertise often lies in other disease-relevant areas.

Our work also has methodological limitations. For example, we have included multi-center human data, but only single center mouse data. While our CMAP declines are similar to those reported elsewhere (66), the addition of preclinical data from other laboratories would strengthen the analysis. Furthermore, we have recorded CMAPs in mice using needle electrodes, while surface electrodes are used in human subjects. Comparing differences relative to healthy controls, or relative to a defined starting point, in both mice and patients helps offset this difference. We also saw significant heterogeneity in human data which highlights the importance of having well defined recording protocols in multi-center studies. In human studies, there is also the added complexity of recruiting

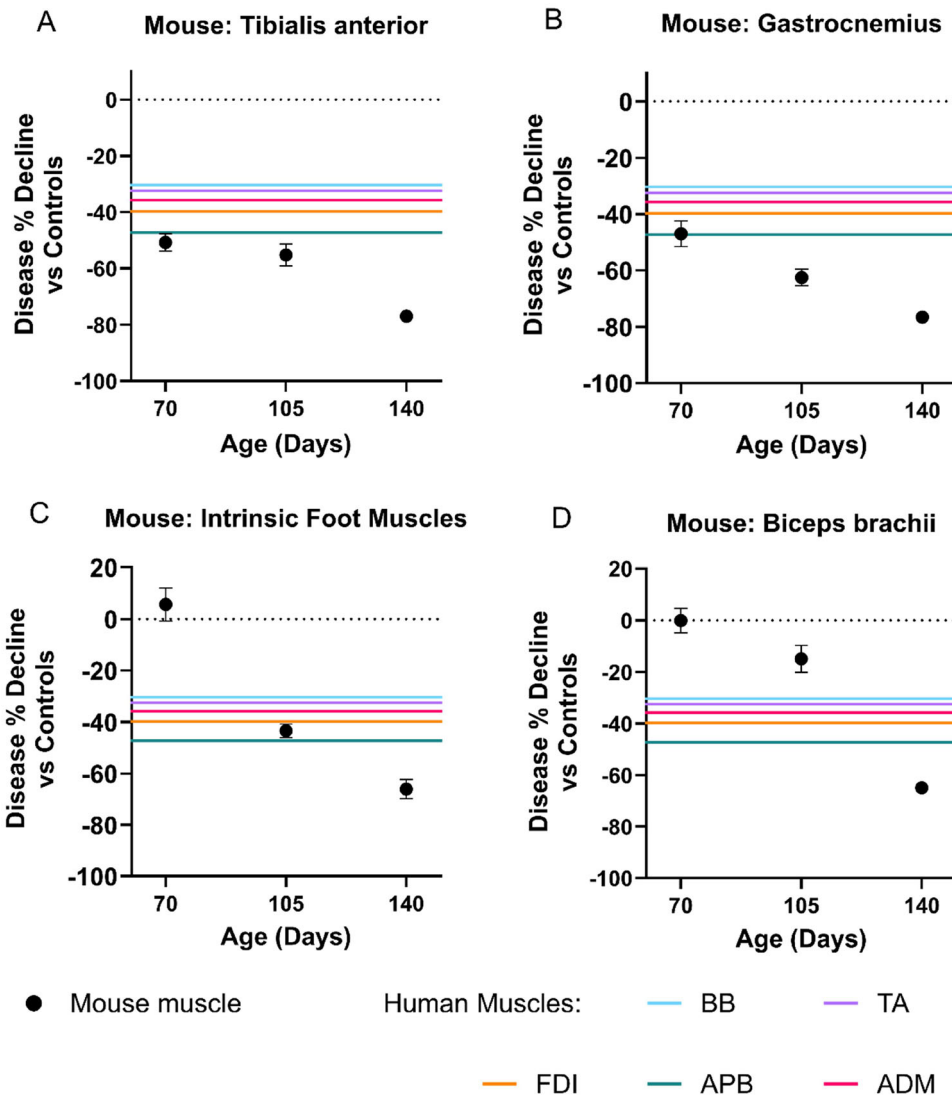


Figure 1. $SOD1^{G93A}$ 70-day tibialis anterior and gastrocnemius CMAP % decline versus healthy controls most resemble human ALS patient versus healthy controls at baseline visit. $SOD1^{G93A}$ mouse data (black circles) is presented as the percentage difference to age-matched non-transgenic controls at three time points (average \pm SEM). Similarly, human data is also presented as the relative difference when compared to age/gender matched healthy volunteers. Data are shown for each mouse muscle (black) studied: tibialis anterior (A), gastrocnemius (B), intrinsic foot muscles (C), and biceps brachii (D), overlaid with patient data for different muscles (colored lines).

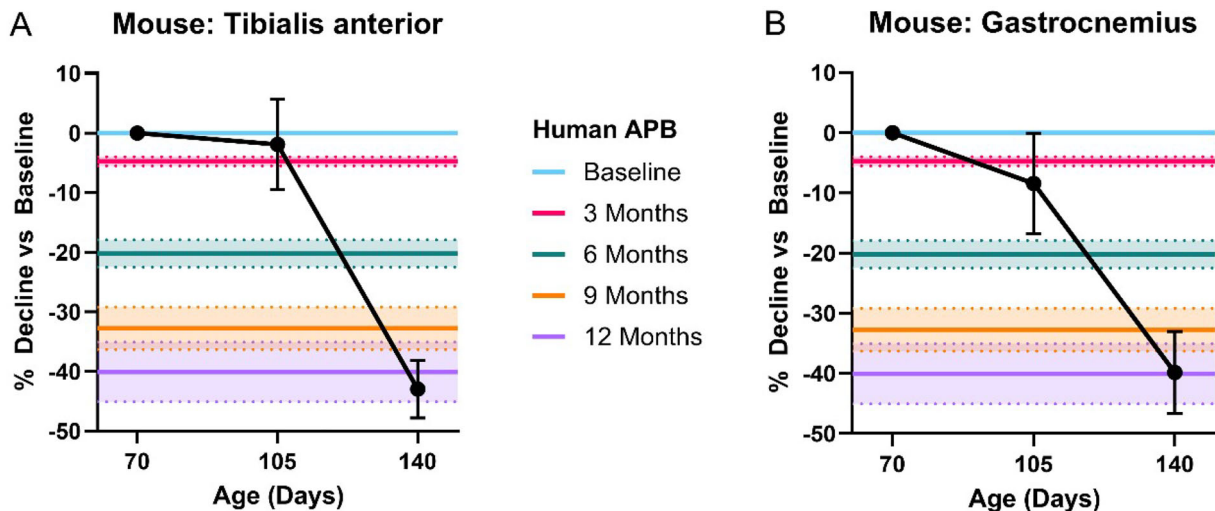


Figure 2. $SOD1^{G93A}$ tibialis anterior and gastrocnemius longitudinal data from P70 to P140 represent a good match to the 12-month decline in human APB. Average (\pm SEM) CMAP decline compared to baseline recording at three time points in the $SOD1^{G93A}$ mouse (black circles) in tibialis anterior (A) and gastrocnemius (B). The different time points in human APB are represented by horizontal colored lines (mean represented by the line and standard error by the shaded area).

patients at different stages of disease and with different disease trajectories. Recent modeling work has demonstrated several different patterns of ALSFRS-R decline (67) and it is likely that there are several different patterns of decline in other measures of disease too. In contrast, our simple approach only relates the mean of one group to the mean of another. However, this approach can provide a starting point for more sophisticated attempts to reconcile preclinical and clinical disease measurement.

We suggest that translational biomarkers can have a key role to play in the design of preclinical studies. Clearly, the use of “survival” in the SOD1G93A model has been particularly unreliable as a predictor of clinical efficacy. By attempting to directly relate preclinical data to patient data using the same readout as we have done, preclinical studies can identify when the most clinically relevant starting point might be for the outcome measures being used. If therapeutics are shown to reduce CMAP decline in mouse models, clinical studies could be designed to incorporate CMAPs as a primary or secondary endpoint allowing a direct comparison for therapeutic effects. In addition, it may enable better predictions of treatment effect sizes for calculating clinical studies sample sizes. Incorporating CMAP amplitudes into the inclusion/exclusion criteria would then be necessary to ensure that a potential amenable to monitoring was available. In our literature search, CMAP amplitudes generally declined by around 40%, so a pragmatic approach might be to specify an amplitude of 2 mV for certain nerves, to ensure a reliable potential was likely to be present for the duration of the study (accepting faster progression may mean this is not the case). With further development, such approaches may be able to build confidence in the preclinical data package for successful translation of neuroprotective approaches into ALS clinical trials.

Author contributions

S.M., A.K., and T.W. conducted the animal experiments. S.M. analysed the mouse CMAP data. Z.Q. and J.A. conducted the review, data extraction and analysis of the clinical studies. P.J.S., J.J.P.A. and R.J.M. designed the study, supervised the work. R.J.M. obtained the funding. S.M., J.J.P.A., and R.J.M. drafted the manuscript. All authors reviewed and edited the manuscript.

Declaration of interest

The authors report no conflicts of interest. The authors alone are responsible for the content and writing of this article. This work was funded by Nxera Pharma UK Ltd.

Data availability statement

The datasets analyzed for human data are cited. Mouse data available on request.

References

1. Van Den Bosch L, Tilkin P, Lemmens G, Robberecht W. Minocycline delays disease onset and mortality in a transgenic model of ALS. *Neuroreport*. 2002;13:1067–70.
2. Cudkowicz ME, Shefner JM, Schoenfeld DA, Zhang H, Andreasson KI, Rothstein JD, et al. Trial of celecoxib in amyotrophic lateral sclerosis. *Ann Neurol*. 2006;60:22–31.
3. Drachman DB, Frank K, Dykes-Hoberg M, Teismann P, Almer G, Przedborski S, et al. Cyclooxygenase 2 inhibition protects motor neurons and prolongs survival in a transgenic mouse model of ALS. *Ann Neurol*. 2002;52:771–8.
4. Gordon PH, Moore DH, Miller RG, Florence JM, Verheijde JL, Doorish C, et al. Efficacy of minocycline in patients with amyotrophic lateral sclerosis: a phase III randomised trial. *Lancet Neurol*. 2007;6:1045–53.
5. Groeneveld GJ, Veldink JH, van der Tweel I, Kalmijn S, Beijer C, de Visser M, et al. A randomized sequential trial of creatine in amyotrophic lateral sclerosis. *Ann Neurol*. 2003;53:437–45.
6. Snow RJ, Turnbull J, da Silva S, Jiang F, Tarnopolsky MA. Creatine supplementation and riluzole treatment provide similar beneficial effects in copper, zinc superoxide dismutase (G93A) transgenic mice. *Neuroscience*. 2003;119:661–7.
7. Ito H, Wate R, Zhang J, Ohnishi S, Kaneko S, Ito H, et al. Treatment with edaravone, initiated at symptom onset, slows motor decline and decreases SOD1 deposition in ALS mice. *Exp Neurol*. 2008;213:448–55.
8. McCampbell A, Cole T, Wegener AJ, Tomassy GS, Setnicka A, Farley BJ, et al. Antisense oligonucleotides extend survival and reverse decrement in muscle response in ALS models. *J Clin Invest*. 2018;128:3558–67.
9. Stephenson J, Amor S. Modelling amyotrophic lateral sclerosis in mice. *Drug Discov Today Dis Model*. 2017;25–26:35–44.
10. White MA, Lin Z, Kim E, et al. Sarm1 deletion suppresses TDP-43-linked motor neuron degeneration and cortical spine loss. *Acta Neuropathol Commun*. 2019;7:1–16.
11. Watkins JA, Alix JJP, Shaw PJ, Mead RJ. Extensive phenotypic characterisation of a human TDP-43Q331K transgenic mouse model of amyotrophic lateral sclerosis (ALS). *Sci Rep*. 2021;11:16659.
12. Devoy A, Kalmar B, Stewart M, Park H, Burke B, Noy SJ, et al. Humanized mutant FUS drives progressive motor neuron degeneration without aggregation in “FUSDelta14” knockin mice. *Brain*. 2017;140:2797–805.
13. Gurney ME, Pu H, Chiu AY, Dal Canto MC, Polchow CY, Alexander DD, et al. Motor neuron degeneration in mice that express a human Cu, Z. *Science*. 1994;264:1772–5.
14. Mead RJ, Bennett EJ, Kennerley AJ, Sharp P, Sunyach C, Kasher P, et al. Optimised and rapid pre-clinical screening in the SOD1 G93A transgenic mouse model of amyotrophic lateral sclerosis (ALS). *PLOS One*. 2011;6:e23244.
15. Liu Y, Pattamatta A, Zu T, Reid T, Bardhi O, Borchelt DR, et al. C9orf72 BAC mouse model with motor deficits and neurodegenerative features of ALS/FTD. *Neuron*. 2016;90:521–34.
16. Mordes DA, Morrison BM, Ament XH, Cantrell C, Mok J, Eggen P, et al. Absence of survival and motor deficits in

- 500 repeat C9ORF72 BAC mice. *Neuron*. 2020;108:775–83.e4.
17. Andrews JA, Bruijn LI, Shefner JM. ALS drug development guidances and trial guidelines: consensus and opportunities for alignment. *Neurology*. 2019;93:66–71.
 18. Scott S, Kranz JE, Cole J, Linceum JM, Thompson K, Kelly N, et al. Design, power, and interpretation of studies in the standard murine model of ALS. *Amyotroph Lateral Scler*. 2008;9:4–15.
 19. Berry JD, Miller RA, Moore DH, Cudkowicz ME, van den Berg LH, Kerr DA, et al. The combined assessment of function and survival (CAFS): a new endpoint for ALS clinical trials. *Amyotroph Lateral Scler Frontotemporal Degener*. 2013;14:162–8.
 20. Benmouna K, Milants C, Wang FC. Correlations between MUNIX and adapted multiple point stimulation MUNE methods. *Clin Neurophysiol*. 2018;129:341–4.
 21. Jacobsen AB, Bostock H, Tankisi H. CMAP Scan MUNE (MScan)—a novel motor unit number estimation (MUNE) method. *J Vis Exp*. 2018;2018:1–7.
 22. Kristensen RS, Bostock H, Tan SV, Witt A, Fuglsang-Frederiksen A, Qerama E, et al. MScanFit motor unit number estimation (MScan) and muscle velocity recovery cycle recordings in amyotrophic lateral sclerosis patients. *Clin Neurophysiol*. 2019;130:1280–8.
 23. Jenkins TM, Alix JJP, David C, Pearson E, Rao DG, Hoggard N, et al. Imaging muscle as a potential biomarker of denervation in motor neuron disease. *J Neurol Neurosurg Psychiatry*. 2018;89:248–55.
 24. Jenkins TM, Alix JJP, Fingret J, Esmail T, Hoggard N, Baster K, et al. Longitudinal multi-modal muscle-based biomarker assessment in motor neuron disease. *J Neurol*. 2020;267:244–56.
 25. Pollari E, Prior R, Robberecht W, et al. In vivo electrophysiological measurement of compound muscle action potential from the forelimbs in mouse models of motor neuron degeneration. *J Vis Exp*. 2018;2018:1–6.
 26. Mancuso R, Osta R, Navarro X. Presymptomatic electrophysiological tests predict clinical onset and survival in SOD1G93A ALS mice. *Muscle Nerve*. 2014;50:943–9.
 27. Khan HA. Impaired nerve conduction velocity in MPTP-treated mouse model of Parkinson's disease. *Int J Neurosci*. 2015;125:361–6.
 28. Krus KL, Strickland A, Yamada Y, Devault L, Schmidt RE, Bloom AJ, et al. Loss of Stathmin-2, a hallmark of TDP-43-associated ALS, causes motor neuropathy. *Cell Rep*. 2022;39:111001.
 29. Alix JJP, Plesia M, Shaw PJ, Mead RJ, Day JCC. Combining electromyography and Raman spectroscopy: optical EMG. *Muscle Nerve*. 2023;68:464–70.
 30. Watkins J, Ghosh A, Keerie AFA, Alix JJP, Mead RJ, Sreedharan J, et al. Female sex mitigates motor and behavioural phenotypes in TDP-43Q331K knock-in mice. *Sci Rep*. 2020;10:19220.
 31. Keerie A, Brown-Wright H, Kirkland I, Grierson A, Alix JJP, Holscher C, et al. The GLP-1 receptor agonist, liraglutide, fails to slow disease progression in SOD1G93A and TDP-43Q331K transgenic mouse models of ALS. *Sci Rep*. 2021;11:17027.
 32. Maathuis EM, Drenthen J, van Doorn PA, Visser GH, Blok JH. The CMAP scan as a tool to monitor disease progression in ALS and PMA. *Amyotroph Lateral Scler Frontotemporal Degener*. 2013;14:217–23.
 33. Cheah BC, Lin CSY, Park SB, Vucic S, Krishnan AV, Kiernan MC, et al. Progressive axonal dysfunction and clinical impairment in amyotrophic lateral sclerosis. *Clin Neurophysiol*. 2012;123:2460–7.
 34. De Carvalho M, Swash M. Sensitivity of electrophysiological tests for upper and lower motor neuron dysfunction in ALS: a six-month longitudinal study. *Muscle and Nerve*. 2010;41:208–11.
 35. Simon NG, Lagopoulos J, Paling S, Pfluger C, Park SB, Howells J, et al. Peripheral nerve diffusion tensor imaging as a measure of disease progression in ALS. *J Neurol*. 2017;264:882–90.
 36. Chan Y, Alix JJP, Neuwirth C, Barkhaus PE, Castro J, Jenkins TM, et al. Reinnervation as measured by the motor unit size index is associated with preservation of muscle strength in amyotrophic lateral sclerosis, but not all muscles reinnervate. *Muscle Nerve*. 2022;65:203–10.
 37. Yuen EC, Olney RK. Longitudinal study of fiber density and motor unit number estimate in patients with amyotrophic lateral sclerosis. *Neurology*. 1997;49:573–8.
 38. Smith BN, Ticozzi N, Fallini C, Gkazi AS, Topp S, Kenna KP, et al. Exome-wide rare variant analysis identifies TUBA4A mutations associated with familial ALS. *Neuron*. 2014;84:324–31.
 39. Neuwirth C, Barkhaus PE, Burkhardt C, Castro J, Czell D, de Carvalho M, et al. Tracking motor neuron loss in a set of six muscles in amyotrophic lateral sclerosis using the Motor Unit Number Index (MUNIX): a 15-month longitudinal multicentre trial. *J Neurol Neurosurg Psychiatry*. 2015;86:1172–9.
 40. Wang Z-L, Liu M, Ding Q, Hu Y, Cui L. Split-hand index in amyotrophic lateral sclerosis: an F-wave study. *Amyotroph Lateral Scler Frontotemporal Degener*. 2019;20:562–7.
 41. Paparella G, Ceccanti M, Colella D, Cannavacciuolo A, Guerra A, Inghilleri M, et al. Bradykinesia in motoneuron diseases. *Clin Neurophysiol*. 2021;132:2558–66.
 42. Escorcio-Bezerra ML, Abrahao A, de Castro I, Chieia MAT, de Azevedo LA, Pinheiro DS, et al. MUNIX: reproducibility and clinical correlations in amyotrophic lateral sclerosis. *Clin Neurophysiol*. 2016;127:2979–84.
 43. Kim D-G, Hong Y-H, Shin J-Y, Park KH, Sohn S-Y, Lee K-W, et al. Split-hand phenomenon in amyotrophic lateral sclerosis: a motor unit number index study. *Muscle Nerve*. 2016;53:885–8.
 44. Zheng C, Zhu Y, Shao M, Zhu D, Hu H, Qiao K, et al. Split-hand phenomenon quantified by the motor unit number index for distinguishing cervical spondylotic amyotrophy from amyotrophic lateral sclerosis. *Neurophysiol Clin*. 2019;49:391–404.
 45. Shibuya K, Park SB, Geevasinga N, Menon P, Howells J, Simon NG, et al. Motor cortical function determines prognosis in sporadic ALS. *Neurology*. 2016;87:513–20.
 46. Singh R-J, Preethish-Kumar V, Polavarapu K, Vengalil S, Prasad C, Nalini A, et al. Reverse split hand syndrome: dissociated intrinsic hand muscle atrophy pattern in Hirayama disease/brachial monomelic amyotrophy. *Amyotroph Lateral Scler Frontotemporal Degener*. 2017;18:10–6.
 47. Sharma KR, Miller RG. Electrical and mechanical properties of skeletal muscle underlying increased fatigue in patients with amyotrophic lateral sclerosis. *Muscle Nerve*. 1996;19:1391–400.
 48. Min YG, Choi S-J, Hong Y-H, Kim S-M, Shin J-Y, Sung J-J, et al. Dissociated leg muscle atrophy in amyotrophic lateral sclerosis/motor neuron disease: the 'split-leg' sign. *Sci Rep*. 2020;10:15661.
 49. Sun X, Zhang Z, Liu N. Absence of split hand in the flail arm variant of ALS. *Neurophysiol Clin*. 2016;46:149–52.
 50. Oguz-Akarsu E, Sirin NG, Artug T, Erbas B, Kocasoy Orhan E, Idrisoglu HA, et al. Automatic detection of F waves and F-MUNE in two types of motor neuron diseases. *Muscle Nerve*. 2022;65:422–32.
 51. Iwai Y, Shibuya K, Misawa S, Sekiguchi Y, Watanabe K, Amino H, et al. Axonal dysfunction precedes motor neuronal death in amyotrophic lateral sclerosis. *PLOS One*. 2016;11:e0158596.
 52. Fang J, Cui L, Liu M, Guan Y, Li X, Li D, et al. Differences in dysfunction of thenar and hypothenar

- motoneurons in amyotrophic lateral sclerosis. *Front Hum Neurosci.* 2016;10:99.
53. Fang J, Liu M-S, Guan Y-Z, Du H, Li B-H, Cui B, et al. Pattern differences of small hand muscle atrophy in amyotrophic lateral sclerosis and mimic disorders. *Chin Med J.* 2016;129:792–8.
 54. Deilami P, Ghourchian S, Ashtiani BH, Esmaeili S, Bahadori M, Shojaee SF, et al. Correlations between median nerve sonography and conduction study results and functional scales in amyotrophic lateral sclerosis. *Acta Med Iran.* 2019;57:658–62.
 55. Gunes T, Sirin NG, Sahin S, Kose E, Isak B. Use of CMAP, MScan fit-MUNE, and MUNIX in understanding neurodegeneration pattern of ALS and detection of early motor neuron loss in daily practice. *Neurosci Lett.* 2021; 741:135488.
 56. Shimizu T, Bokuda K, Kimura H, Kamiyama T, Nakayama Y, Kawata A, et al. Sensory cortex hyperexcitability predicts short survival in amyotrophic lateral sclerosis. *Neurology.* 2018;90:e1578–e87.
 57. Boekestein WA, Schelhaas HJ, van Putten MJAM, Stegeman DF, Zwarts MJ, van Dijk JP, et al. Motor unit number index (MUNIX) versus motor unit number estimation (MUNE): a direct comparison in a longitudinal study of ALS patients. *Clin Neurophysiol.* 2012;123: 1644–9.
 58. Hviid CVB, Madsen AT, Winther-Larsen A. Biological variation of serum neurofilament light chain. *Clin Chem Lab Med.* 2022;60:569–75.
 59. Corcia P, Bede P, Pradat P-F, Couratier P, Vucic S, de Carvalho M, et al. Split-hand and split-limb phenomena in amyotrophic lateral sclerosis: pathophysiology, electrophysiology and clinical manifestations. *J Neurol Neurosurg Psychiatry.* 2021;92:1126–30.
 60. Seyhan AA. Lost in translation: the valley of death across preclinical and clinical divide – identification of problems and overcoming obstacles. *Transl Med Commun.* 2019;4: 1–19.
 61. Turner MR, Kiernan MC, Leigh PN, Talbot K. Biomarkers in amyotrophic lateral sclerosis. *Lancet Neurol.* 2009;8:94–109.
 62. Verber NS, Shephard SR, Sassani M, McDonough HE, Moore SA, Alix JJP, et al. Biomarkers in motor neuron disease: a state of the art review. *Front Neurol.* 2019;10: 291.
 63. Boylan K, Yang C, Crook J, Overstreet K, Heckman M, Wang Y, et al. Immunoreactivity of the phosphorylated axonal neurofilament H subunit (pNF-H) in blood of ALS model rodents and ALS patients: evaluation of blood pNF-H as a potential ALS biomarker. *J Neurochem.* 2009;111:1182–91.
 64. Lu C-H, Petzold A, Kalmar B, Dick J, Malaspina A, Greensmith L, et al. Plasma neurofilament heavy chain levels correlate to markers of late stage disease progression and treatment response in SOD1G93A mice that model ALS. *PLOS One.* 2012;7:e40998.
 65. Shefner JM, Cudkovic ME, Brown RH. Comparison of incremental with multipoint MUNE methods in transgenic ALS mice. *Muscle Nerve.* 2002;25:39–42.
 66. Mancuso R, Santos-Nogueira E, Osta R, Navarro X. Electrophysiological analysis of a murine model of motoneuron disease. *Clin Neurophysiol.* 2011;122:1660–70.
 67. Ramamoorthy D, Severson K, Ghosh S, Sachs K, Glass JD, Fournier CN, et al. Identifying patterns in amyotrophic lateral sclerosis progression from sparse longitudinal data. *Nat Comput Sci.* 2022;2:605–16.